

tation and explanation of attenuation poles of a dual-mode dielectric-resonator bandpass filter, *IEEE Trans Microwave Theory Tech* 46 (1998), 2159–2163.

5. L. Zhu, P. Wecowski, and K. Wu, New planar dual-mode filter using cross-slotted patch resonator for simultaneous size and loss reduction, *IEEE Trans Microwave Theory Tech* 47 (1999), 650–654.
6. J.-S. Hong and M.J. Lancaster, Microstrip triangular patch resonator filters, *IEEE MTT-S Int Microwave Symp Digest* (2000), 331–334.
7. L. Zhu, S. Sun, and W. Menzel, Ultra-wideband (UWB) bandpass filters using multiple-mode resonator, *IEEE Microwave Wireless Compon Lett* 15 (2005), 796–798.
8. K. Ma, K.S. Yeo, J.-G. Ma, and M.A. Do, An ultra-compact hairpin band pass filter with additional zero points, *IEEE Microwave Wireless Compon Lett* 17 (2007), 262–264.
9. K. Ma, J.-G. Ma, M.A. Do, and K.S. Yeo, A novel compact two-order band pass filter with three zero points, *IEE Electron Lett* 41 (2005), 846–848.
10. F. Giannini, R. Sorrentino, and J. Vrba, Planar circuit analysis of microstrip radial stub, *IEEE Trans Microwave Theory Tech* 32 (1984), 1652–1655.
11. F. Giannini, C. Paoloni, and M. Ruggieri, CAD-oriented lossy models for radial stubs, *IEEE Trans Microwave Theory Tech* 36 (1988), 305–313.

© 2009 Wiley Periodicals, Inc.

CHIP-INDUCTOR-EMBEDDED SMALL-SIZE PRINTED STRIP MONOPOLE FOR WWAN OPERATION IN THE MOBILE PHONE

Ting-Wei Kang and Kin-Lu Wong

Department of Electrical Engineering, National Sun Yat-Sen University, Kaohsiung 80424, Taiwan; Corresponding author: kangtw@ema.ee.nsysu.edu.tw

Received 3 August 2008

ABSTRACT: A simple small-size printed strip monopole embedded with a chip inductor for covering all the five operating bands of GSM850/900/1800/1900/UMTS for wireless wide area network (WWAN) operation in the mobile phone is presented. The antenna consists of a chip-inductor-embedded longer radiating strip and a shorter radiating strip. With a 10-nH chip inductor embedded, the longer radiating strip has a length of about 46 mm only (about 0.14 wavelength at 900 MHz), yet supports a wide resonant mode at about 900 MHz for the antenna's lower band to cover GSM850/900 operation. The shorter radiating strip has a length of about 30 mm (about 0.2 wavelength at 2000 MHz) and provides a wide resonant mode at about 2000 MHz for the antenna's upper band to cover GSM1800/1900/UMTS operation. With the five operating bands covered, the two radiating strips occupy a small printed area of about 350 mm² on the system circuit board of the mobile phone. Details of the proposed antenna are described, and the specific absorption rate results of the antenna are also analyzed. © 2009 Wiley Periodicals, Inc. *Microwave Opt Technol Lett* 51: 966–971, 2009; Published online in Wiley InterScience (www.interscience.wiley.com). DOI 10.1002/mop.24225

Key words: internal mobile phone antennas; printed monopoles; WWAN antennas; multiband operation; chip-inductor-embedded antennas

1. INTRODUCTION

Thin mobile phones are recently becoming attractive for mobile users. For applications in the thin mobile phones, it is demanded that the embedded internal antennas should be of thin profile. In

addition, multiband operation covering GSM850 (824–894 MHz), GSM900 (890–960 MHz), GSM1800 (1710–1880 MHz), GSM1900 (1850–1990 MHz), and UMTS (1920–2170 MHz) for wireless wide area network (WWAN) operation is also a must for the promising internal antennas. The reported multiband internal mobile phone antennas such as the planar inverted-F antenna (PIFA) with multiradiating strips [1, 2] or Hilbert-type radiating strips [3], the loop strip antenna [4, 5], and the like, however, show a high profile of about 6–10 mm above the system ground plane of the mobile phone. It is also possible to achieve a lowered profile of about 3–4 mm for the PIFA [6, 7]; however, with which multiband operation for covering all the five operating bands for WWAN operation is difficult to obtain. Another alternative is to use the monopole PIFA (the PIFA with its radiating strips mounted above the top edge of the system ground plane); in this case, a typical case of achieving a small thickness of 4 mm for the antenna has been reported [8].

Another promising alternative for achieving the thin internal mobile phone antenna is by printing the antenna's radiating strips directly on the top no-ground or bottom no-ground portion on the system circuit board of the mobile phone, such as the multiband printed loop mobile phone antenna [9, 10] and the multiband printed slot or monopole slot (quarter-wavelength slot) mobile phone antenna [11–13]. In this case, the thickness of the antenna is reduced to be minimum, especially for the design of printing on one side of the system circuit board only. In this article, we demonstrate another promising printed internal mobile phone antenna with a simple and reduced-size structure, yet capable of covering GSM850/900/1800/1900/UMTS for pentaband WWAN operation. Different from the printed antennas in [9–13], the proposed antenna in this study is a small-size strip monopole formed by two printed radiating strips of a chip-inductor-embedded longer radiating strip and a shorter radiating strip. The embedded inductor can lead to the size reduction of the antenna [14]. The additional inductance contributed by the embedded inductor can compensate for the increased capacitance resulting from the decreased length of the radiating strip. Hence, the longer radiating strip with a small mean length of about 0.14 wavelength at 900 MHz in this study can generate a wide operating band for the antenna's lower band to cover GSM850/900 operation. The shorter radiating strip of about 0.2 wavelength at 2000 MHz can be placed close to the longer radiating strip to occupy a compact area on the system circuit board of the mobile phone, resulting in small effects on the antenna's lower band and also generating an additional resonant mode at about 2000 MHz for the antenna's upper band to cover GSM1800/1900/UMTS operation. Detailed design considerations of the proposed antenna are described in the article. Also, the proposed printed antenna can be placed either at the top or bottom position on the system circuit board of the mobile phone for practical applications. For the two possible positions, the specific absorption rate (SAR) results [15–17] of the antenna are also analyzed.

2. PROPOSED SMALL-SIZE STRIP MONOPOLE

Figure 1 shows the geometry of the proposed small-size printed strip monopole embedded with a chip inductor for WWAN operation in the mobile phone. The proposed antenna is printed on the top no-ground portion (size 15×60 mm²) of the system circuit board of size 115×60 mm². A 0.8-mm-thick FR4 substrate of relative permittivity 4.4 is used in this study to be treated as the system circuit board, whose dimensions studied here are reasonable for practical personal digital assistant (PDA) phones or smart phones [7, 18, 19]. Below the top no-ground portion shown in

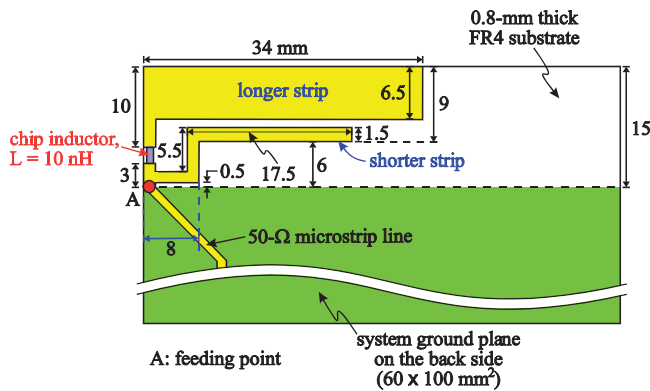


Figure 1 Geometry of the proposed small-size printed strip monopole embedded with a chip inductor for WWAN operation in the mobile phone. [Color figure can be viewed in the online issue, which is available at www.interscience.wiley.com]

Figure 1 is the system ground plane of size $100 \times 60 \text{ mm}^2$. Note that by rotating the system circuit board 180° , the proposed antenna is on the bottom no-ground portion (antenna at the bottom position) as shown in Figure 9. In the case of the antenna at the bottom position, the obtained SAR results from exposure to radiation of the proposed antenna can be greatly decreased. This method of embedding the internal antenna at the bottom position of the mobile phone has been used in some mobile phones for reducing the SAR. The related SAR results will be analyzed in the next section with the aid of Table 1 and Figure 10.

The proposed antenna comprises a longer radiating strip and a shorter radiating strip. The longer strip is embedded with a chip inductor (length 2.0 mm and width 1.2 mm) of 10 nH near its front end at the top edge of the ground plane; this front end is also the antenna's feeding point (point A in the figure). The shorter strip has a uniform width of 1.5 mm and a length of about 30 mm, which is about 0.2 wavelength at 2000 MHz. Owing to the dielectric substrate (the system circuit board) effect, which reduces the required resonant length for the 0.25-wavelength mode, a wide-band resonant mode can be excited at about 2000 MHz for the antenna's upper band to cover GSM1800/1900/UMTS operation.

For the longer strip, it has a mean length of about 46 mm or about 0.14 wavelength at 900 MHz only. With such a short length, however, the longer strip in this study can support a resonant mode normally requiring a length of about 0.25 wavelength at the desired

TABLE 1 Simulated SAR in 1 and 10 g of Head Tissue from Exposure to Radiation of the Proposed Antenna Obtained from SEMCAD [22]

Antenna at the top position					
Frequency (MHz)	859	925	1795	1920	2045
1-g SAR (W/kg)	2.15	1.50	2.64	2.45	2.28
10-g SAR (W/kg)	0.70	0.52	0.85	0.80	0.74
Antenna at the bottom position					
Frequency (MHz)	859	925	1795	1920	2045
1-g SAR (W/kg)	1.19	0.95	0.43	0.41	0.34
10-g SAR (W/kg)	0.44	0.36	0.31	0.28	0.23
SAR difference (in dB) between the top and bottom positions					
Frequency (MHz)	859	925	1795	1920	2045
1-g SAR (W/kg)	-2.6 dB	-2.0 dB	-7.9 dB	-7.7 dB	-8.3 dB
10-g SAR (W/kg)	-2.0 dB	-1.6 dB	-4.4 dB	-4.5 dB	-5.1 dB

The system circuit board on which the antenna is printed is spaced 5 mm away from the head phantom.

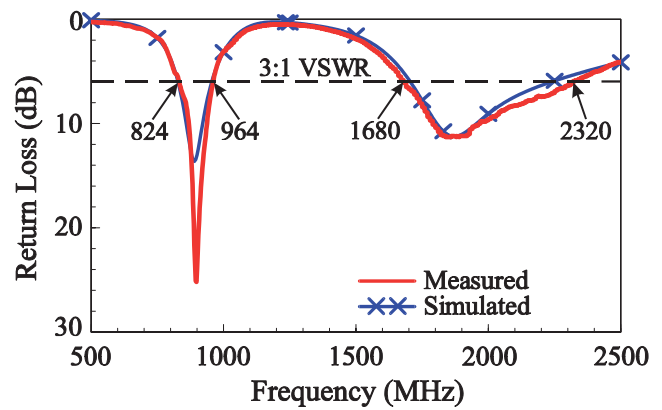


Figure 2 Measured and simulated return loss for the proposed antenna. [Color figure can be viewed in the online issue, which is available at www.interscience.wiley.com]

operating frequency. In addition to the dielectric substrate effect, which reduces the required resonant length, the major effect is owing to the presence of the embedded chip inductor, which contributes additional inductance to compensate for the increased capacitance resulting from the decreased length of the radiating strip. By increasing the inductance of the embedded inductor, the excited resonant mode of the longer strip can also be shifted to lower frequencies. However, the achievable operating bandwidth will also be decreased. More detailed results are shown in Figure 5 for discussion in the next section. Also note that the open-end section of the longer strip is widened to have a width of 6.5 mm, which is helpful for achieving improved impedance matching over the desired operating band [20].

Both the longer and shorter strips can also be incorporated close to each other to have a compact structure. In this study, the two strips together occupy a small printed area of about 354 mm^2 ($9 \times 34 + 6 \times 8 \text{ mm}^2$) on the system circuit board. Hence, the proposed antenna not only shows a simple configuration but also occupies a compact area, allowing it to fabricate at low cost for practical applications. For testing the antenna in the experiment, a 50-Ω microstrip line printed on the front side of the circuit board is used.

3. RESULTS AND DISCUSSION

Figure 2 shows the measured and simulated return loss for the fabricated prototype. Two wide operating bands at about 900 and 2000 MHz are excited with acceptable impedance matching of 3:1 VSWR, which is generally used for the internal WWAN antennas for practical applications in the mobile phone. Good agreement between the measured data and the simulated results obtained using Ansoft HFSS [21] is also seen. The measured impedance bandwidths reach 140 (824–964 MHz) and 640 MHz (1680–2320 MHz) for the antenna's lower and upper bands, respectively. The obtained bandwidths allow the antenna to cover GSM850/900/1800/1900/UMTS for WWAN operation.

Figure 3 shows the comparison of the simulated return loss for the proposed antenna and the reference antenna (the corresponding design without the chip inductor shown in the figure). Without the embedded chip inductor, two resonant modes are also excited for the reference antenna; however, the lower band is centered at about 1250 MHz, much higher than that of the proposed antenna. The embedded chip inductor effectively shifts the lower band to occur at about 900 MHz for GSM850/900 operation. It is interesting to

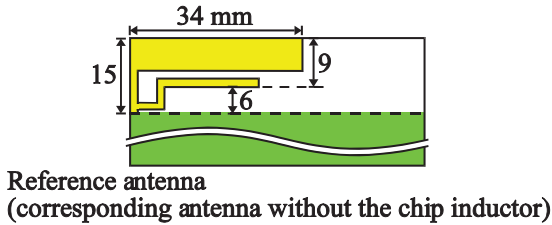
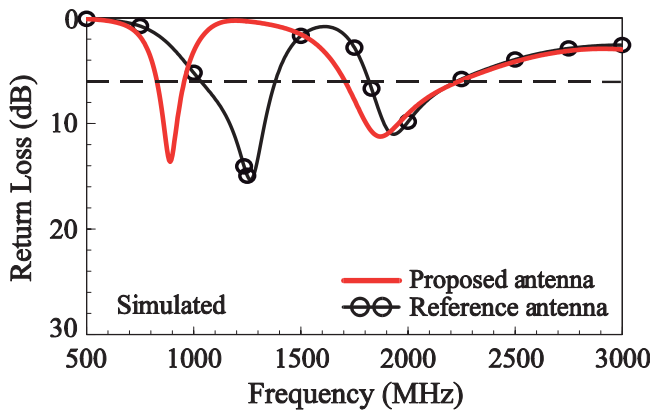


Figure 3 Simulated return loss for the proposed antenna and the reference antenna (the corresponding design without the chip inductor). [Color figure can be viewed in the online issue, which is available at www.interscience.wiley.com]

note that the operating bandwidth of the upper band is also improved with the presence of the chip inductor.

A comparison of the simulated return loss for the proposed antenna, the case with the longer strip only, and the case with the shorter strip only is shown in Figure 4. It is clearly seen that the longer strip controls the antenna's lower band, whereas the shorter strip governs the upper band. Also note that the bandwidths of the two cases of the longer strip only and the shorter strip only are wider than their corresponding resonant mode in the proposed antenna. This bandwidth decrease is largely owing to the coupling effects between the longer and shorter strips arranged to be close to each other for achieving a compact structure.

The simulated return loss as a function of the inductance L of the embedded chip inductor in the proposed antenna is shown in Figure 5. Results of the inductance L varied from 12 to 8.2 nH are

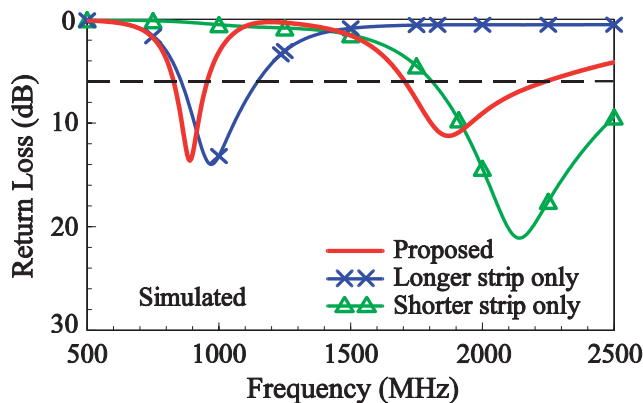


Figure 4 Simulated return loss for the proposed antenna, the case with the longer strip only, and the case with the shorter strip only. [Color figure can be viewed in the online issue, which is available at www.interscience.wiley.com]

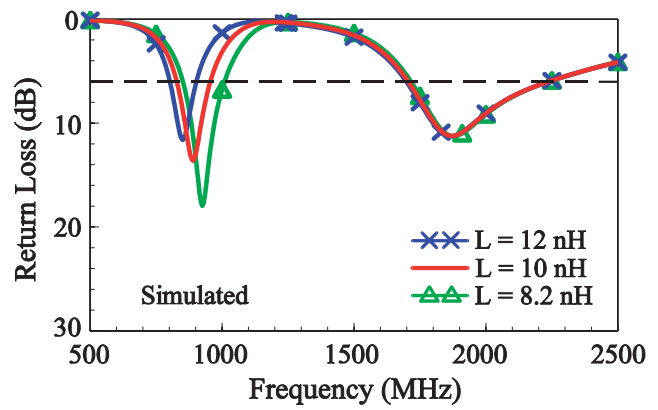


Figure 5 Simulated return loss as a function of the inductance L of the embedded chip inductor. [Color figure can be viewed in the online issue, which is available at www.interscience.wiley.com]

presented. With the increasing inductance, the lower band is shifted to lower frequencies; however, the bandwidth is also slightly decreased. For the upper band, it is almost not affected by the variations in the inductance L .

Figure 6 plots the measured two-dimensional (2D) and three-dimensional (3D) radiation patterns at 859 and 925 MHz, central frequencies of the GSM850 and GSM900 bands, for the fabricated prototype. Similar monopole-like radiation patterns for the two frequencies are observed. Near-omnidirectional radiation in the azimuthal plane (x - y plane) is also seen. The measured 2D and 3D radiation patterns at 1795, 1920, and 2045 MHz (central frequencies of the GSM1800, GSM1900, and UMTS bands) are plotted in

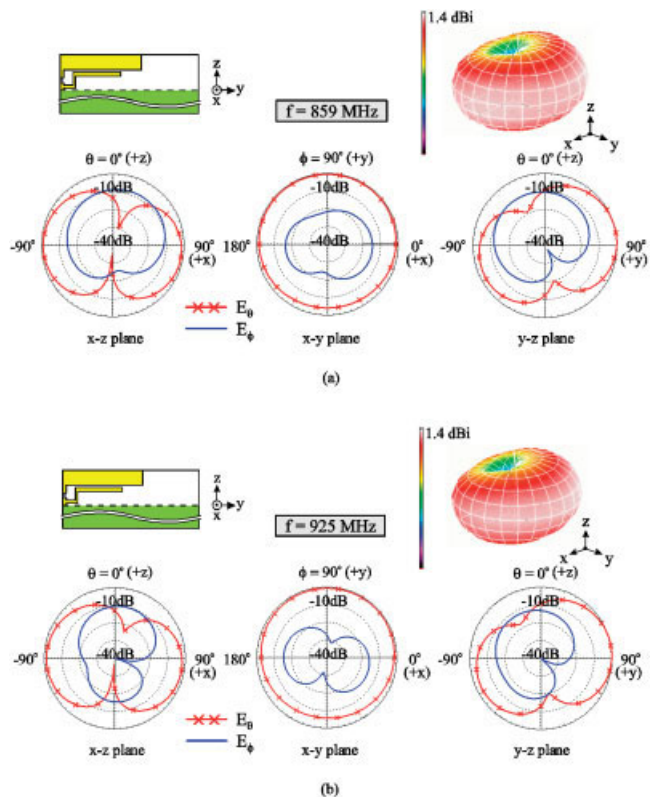


Figure 6 Measured 2D and 3D radiation patterns at (a) 859 MHz and (b) 925 MHz for the proposed antenna. [Color figure can be viewed in the online issue, which is available at www.interscience.wiley.com]

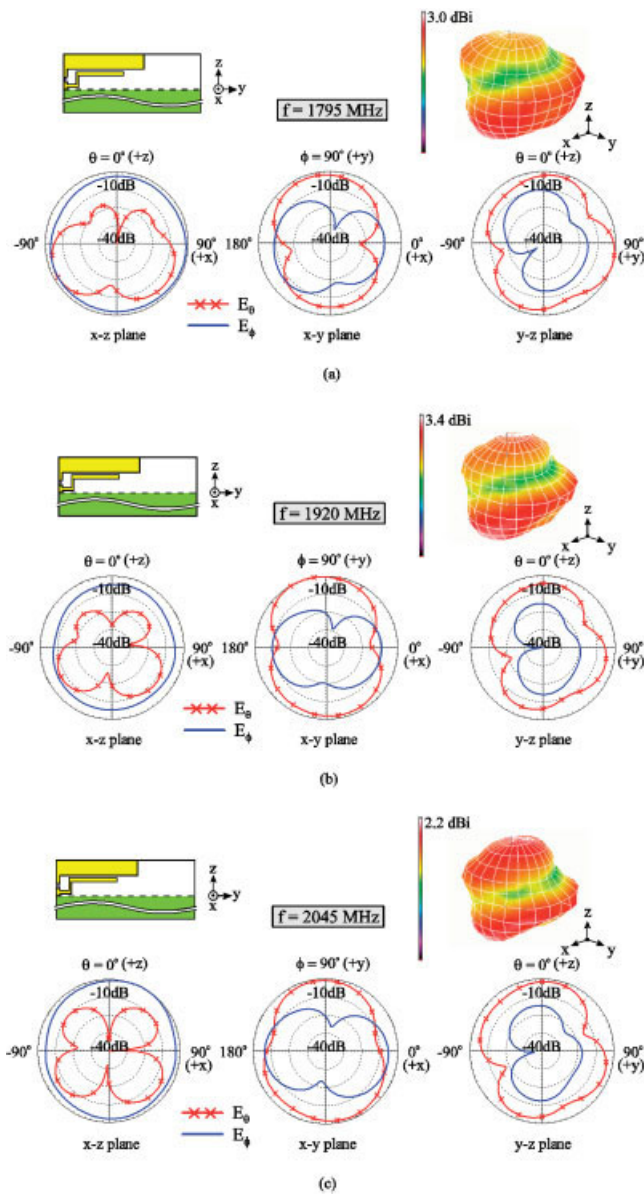
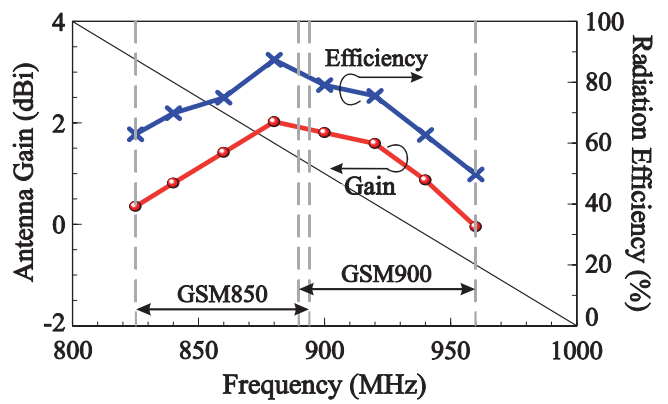


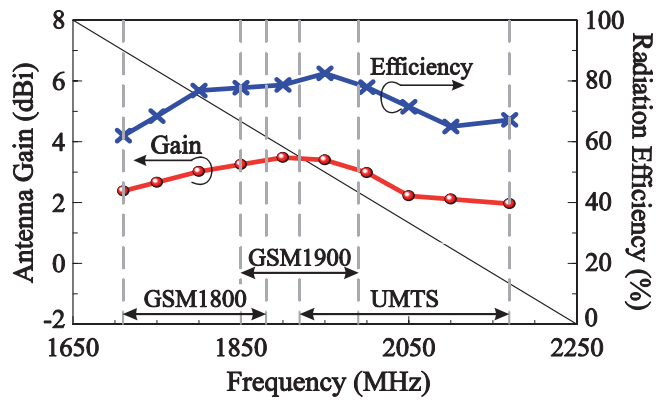
Figure 7 Measured 2D and 3D radiation patterns at (a) 1795 MHz, (b) 1920 MHz, and (c) 2045 MHz for the proposed antenna. [Color figure can be viewed in the online issue, which is available at www.interscience.wiley.com]

Figure 7. The radiation patterns are stable for frequencies over the upper band. In general, the measured radiation patterns show no special distinctions when compared with those observed for the conventional internal mobile phone antennas such as the internal PIFAs [1, 2]. Figure 8 presents the measured antenna gain and radiation efficiency for the fabricated prototype. Over the GSM850/900 band shown in Figure 8(a), the antenna gain is varied from about 0 to 2 dBi, while the radiation efficiency is about 50–87%. Figure 8(b) shows the results over the GSM1800/1900/UMTS band. The antenna gain is varied from about 1.9 to 3.4 dBi, and the radiation efficiency ranges from about 62 to 82%.

The SAR results for the proposed antenna are also analyzed. Figure 9 shows the SAR simulation model for the antenna placed at the top and bottom positions with the head phantom provided by SEMCAD [22]. The simulated SAR results in 1 and 10 g of head tissue from exposure to the antenna radiation are listed in Table 1. Results for the two cases of the top and bottom positions are



(a)



(b)

Figure 8 Measured antenna gain and radiation efficiency for the proposed antenna. (a) GSM850/900 band, (b) GSM1800/1900/UMTS band. [Color figure can be viewed in the online issue, which is available at www.interscience.wiley.com]

presented. For the 10-g SAR results, they all meet the SAR limit of 2.0 W/kg [17] for both cases of the top and bottom positions. For the 1-g SAR results, however, the obtained results exceed the SAR limit of 1.6 W/kg [17] for the top-position case. By placing the antenna at the bottom position, large SAR decrease compared to that at the top position is obtained. Figure 10 shows the simu-

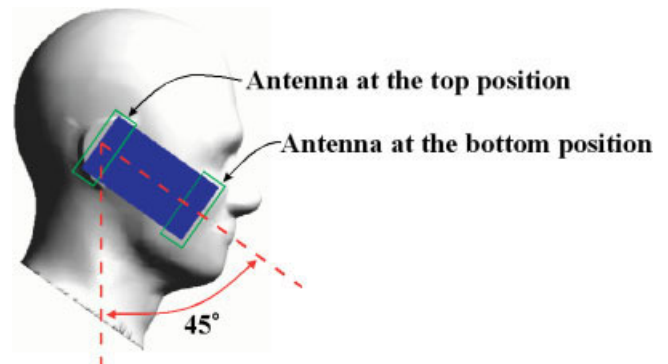


Figure 9 SAR simulation model for the antenna at the top and bottom positions with the head phantom provided by SEMCAD [22]. [Color figure can be viewed in the online issue, which is available at www.interscience.wiley.com]

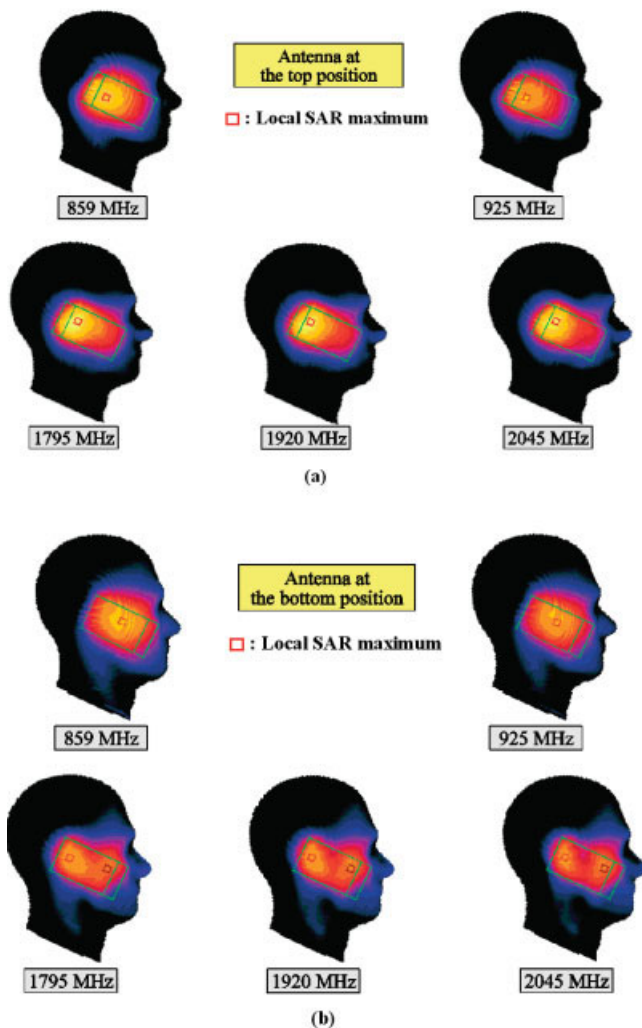


Figure 10 Simulated SAR distributions in 1 g of head tissue from exposure to radiation of the proposed antenna. (a) Antenna at the top position, (b) antenna at the bottom position. [Color figure can be viewed in the online issue, which is available at www.interscience.wiley.com]

lated SAR distributions in 1 g of head tissue for comparison. The open square marks in the figure represent the local SAR maximum or hot spot. It is seen that for lower frequencies at 859 and 925 MHz, the hot spot is moved from near the ear for the top-position case down to the cheek for the bottom-position case, and the hot spot is also weaker for the bottom-position case than the top-position case. For higher frequencies at 1795, 1920, and 2045 MHz, there are two hot spots observed for the bottom-position case, whereas there is only one hot spot for the top-position case. This indicates that the radiation energy is more uniformly distributed for the bottom-position case, and hence leading to decreased SAR values [15]. The results suggest that the proposed antenna is promising to be mounted at the bottom position of the mobile phone for practical applications.

4. CONCLUSIONS

A small-size printed strip monopole suitable for WWAN operation in the mobile phone has been proposed. The antenna is easy to fabricate at low cost on the system circuit board of the mobile phone and shows a simple structure formed by a chip-inductor-embedded longer strip and a shorter strip. Simply by embedding a chip inductor, the longer strip can generate a wideband resonant

mode at about 900 MHz with a length of about 0.14 wavelength at 900 MHz. The generated mode easily covers GSM850/900 operation. The shorter strip, although placed close to the longer strip to achieve a compact structure, can also generate a wideband resonant mode at about 2000 MHz for covering GSM1800/1900/UMTS operation. All the five operating bands for WWAN operation is hence obtained for the proposed antenna. Good radiation characteristics for frequencies over the operating bands have also been obtained. The SAR results for the antenna mounted at the top and bottom positions of the mobile phone have been analyzed. Smaller SAR values meet the SAR limit of 2.0 W/kg in 10-g tissue or 1.6 W/kg in 1-g tissue for the proposed antenna mounted at the bottom position of the mobile phone have been achieved. The obtained results indicate that the proposed antenna is promising for practical applications in the mobile phone for WWAN operation.

REFERENCES

1. K.L. Wong, *Planar antennas for wireless communications*, Wiley, New York, 2003.
2. Y.X. Guo, M.Y.W. Chia, and Z.N. Chen, Miniature built-in multiband antennas for mobile handsets, *IEEE Trans Antennas Propag* 52 (2004), 1936–1944.
3. M.Z. Azad and M. Ali, A miniature Hilbert PIFA for dual-band mobile wireless applications, *IEEE Antennas Wireless Propag Lett* 4 (2005), 59–62.
4. B.K. Yu, B. Jung, H.J. Lee, F.J. Harackiewicz, and B. Lee, A folded and bent internal loop antenna for mobile handset applications, *Microwave Opt Technol Lett* 48 (2006), 463–467.
5. C.I. Lin and K.L. Wong, Internal meandered loop antenna for GSM/DCS multiband operation in a mobile phone with the user's hand, *Microwave Opt Technol Lett* 49 (2007), 759–765.
6. K.L. Wong, Y.C. Lin, and T.C. Tseng, Thin internal GSM/DCS patch antenna for a portable mobile terminal, *IEEE Trans Antennas Propag* 54 (2006), 238–242.
7. K.L. Wong, Y.C. Lin, and B. Chen, Internal patch antenna with a thin air-layer substrate for GSM/DCS operation in a PDA phone, *IEEE Trans Antennas Propag* 55 (2007), 1165–1172.
8. R.A. Bhatti and S.O. Park, Hepta-band internal antenna for personal communication handsets, *IEEE Trans Antennas Propag* 55 (2007), 3398–3403.
9. Y.W. Chi and K.L. Wong, Internal compact dual-band printed loop antenna for mobile phone application, *IEEE Trans Antennas Propag* 55 (2007), 1457–1462.
10. W.Y. Li and K.L. Wong, Internal printed loop-type mobile phone antenna for penta-band operation, *Microwave Opt Technol Lett* 49 (2007), 2595–2599.
11. K.L. Wong, Y.W. Chi, and S.Y. Tu, Internal multiband printed folded slot antenna for mobile phone application, *Microwave Opt Technol Lett* 49 (2007), 1833–1837.
12. C.I. Lin and K.L. Wong, Printed monopole slot antenna for internal multiband mobile phone antenna, *IEEE Trans Antennas Propag* 55 (2007), 3690–3697.
13. C.H. Wu and K.L. Wong, Hexa-band internal printed slot antenna for mobile phone application, *Microwave Opt Technol Lett* 50 (2008), 35–38.
14. T.H. Chang and J.F. Kiang, Meshed antenna reduction by embedding inductors, 2005 IEEE Antennas Propagation Society International Symposium and USNC/URSI National Radio Science Meeting, Washington, DC, USA, Session 78.
15. Z. Li and Y. Rahmat-Samii, Optimization of PIFA-IFA combination in handset antenna design, *IEEE Trans Antennas Propag* 53 (2005), 1770–1778.
16. O. Kivekas, J. Ollikainen, T. Lehtiniemi, and P. Vainikainen, Bandwidth, SAR, and efficiency of internal mobile phone antennas, *IEEE Trans Electromagn Compat* 46 (2004), 71–86.
17. J.C. Lin, Specific absorption rates induced in head tissues by microwave radiation from cell phones, *Microwave & RF* (2001), 22–25.
18. K.L. Wong and C.I. Lin, Internal GSM/DCS antenna backed by a

- step-shaped ground plane for a PDA phone, IEEE Trans Antennas Propag 54 (2006), 2408–2410.
19. K.L. Wong and C.H. Chang, Surface-mountable EMC monopole chip antenna for WLAN operation, IEEE Trans Antennas Propag 54 (2006), 1100–1104.
 20. Y.L. Kuo and K.L. Wong, Printed double-T monopole antenna for 2.4/5.2 GHz dual-band WLAN operations, IEEE Trans Antennas Propag 51 (2003), 2187–2192.
 21. Ansoft Corporation HFSS, Available at: <http://www.ansoft.com/products/hf/hfss/>.
 22. SEMCAD, Schmid & Partner Engineering AG (SPEAG), Available at: <http://www.semcad.com>,

© 2009 Wiley Periodicals, Inc.

A RADIO-OVER-FIBER SYSTEM WITH PHOTONICS GENERATED OFDM SIGNALS BY USING DIRECTLY MODULATED LASER

L. Chen, J. Lu, J. He, Z. Dong, and S. Wen

¹ Key Laboratory for Micro/Nano Opto-Electronic Devices of Ministry of Education, Hunan University, Changsha 410082, China; Corresponding author: liliuchen12@vip.163.com

² School of Computer and Communication, Hunan University, Changsha 410082, China

Received 8 August 2008

ABSTRACT: We have experimentally demonstrated a radio-over-fiber system transmitting 2.5 Gbit/s orthogonal frequency division multiplexing (OFDM) signals carried by 40 GHz millimetre-wave. The 40 GHz optical millimeter wave signals were generated by a directed modulation laser driven by the 2.5 Gbit/s electrical OFDM signals carried by 20 GHz RF signals. The power penalty is less than 1 dB power penalty at bit error rate of 10^{-5} after transmission over 20 km standard single mode fiber. © 2009 Wiley Periodicals, Inc. Microwave Opt Technol Lett 51: 971–973, 2009; Published online in Wiley InterScience (www.interscience.wiley.com). DOI 10.1002/mop.24248

Key words: orthogonal frequency division multiplexing (OFDM); optical millimeter wave (mm-wave); radio-over-fiber (ROF); direct-modulation DFB laser

1. INTRODUCTION

The millimetre wave bands would be utilized to meet the requirement for broadband service and overcome the frequency congestion

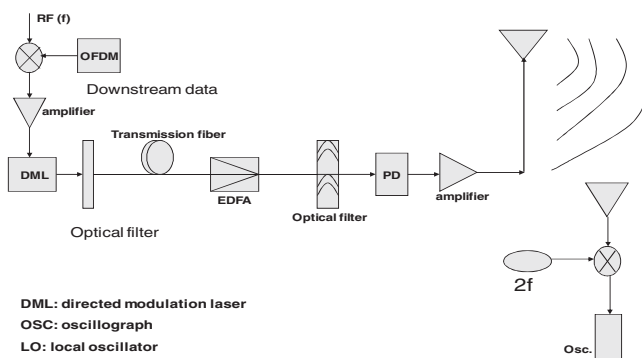


Figure 1 schematic diagram of mm-wave OFDM-ROF system by using directly modulated laser

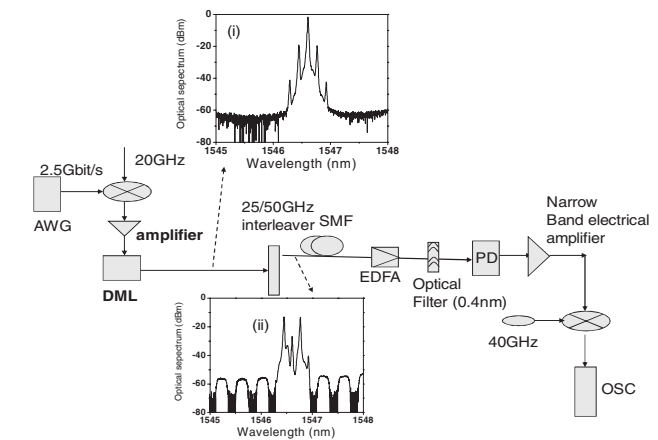


Figure 2 Experimental setup for OFDM-ROF systems. AWG: arbitrary waveform generator; DML: directly modulated laser, PD: photo-detector

tion in the future ROF-based optical-wireless network. In radio-over-fiber (ROF) system, a central station (CS) is connected to many functionally simple base stations (BSs) via optical fiber. Almost all the processes including modulation, demodulation, coding, routing are performed at the CS [1–5]. The main function of BS is to realize optical/electrical conversion and broadcasting by antenna. Orthogonal frequency division multiplexing (OFDM) system can provide excellent tolerance towards multipath delay spread and frequency-dependent channel distortion. Recent research results have demonstrated that OFDM will become a strong candidate for transmission signals in the next generation long-haul and access networks because of its high spectrum efficiency and the resistance to chromatic dispersion and polarization mode dispersion [6–12]. So the combination of OFDM and ROF is naturally suitable for optical-wireless systems to increase the bandwidth and extend the transmission distance of mm-wave over both fiber and air links. The generation of low-cost mm-wave for carrying OFDM signal is one of the key technologies for OFDM-ROF system [7, 8]. Previous investigation for generation of OFDM-mm wave signal is mainly used external modulators, which leads to a complex and expensive configuration. Recently, we have already proposed ROF system based on directly modulated laser to generate optical mm-wave carrying regular OOK signal [13]. In this article, we have experimentally demonstrated a radio-over-fiber system to transmit 2.5 Gbit/s OFDM signals on 40 GHz millimeter wave generated by a directly modulated DFB laser for the first time.

To our knowledge, this is the simplest scheme to generate optical OFDM signal by using directly modulator laser.

2. SYSTEM ARCHITECT

Figure 1 shows the schematic diagram of mm-wave OFDM-ROF system by using directly modulated laser. The OFDM analog data and an RF clock are mixed by using an electrical mixer. The mixed signals are applied to drive a directly modulated laser (DML) to create double sideband (DSB) optical signals. Then an optical filter is employed to separate the first-order sidebands from the optical carrier. The first-order sidebands will be transmitted over SSMF to the base station (BS). In the BS, the mm-wave signal after O/E conversion is broadcasted by an antenna. The received mm-wave signal from the antenna in the customer unit is down-converted to obtain OFDM baseband signal.